Hindawi
Advances in Materials Science and Engineering
Volume 2018, Article ID 7214236, 9 pages
https://doi.org/10.1155/2018/7214236

Research Article

Cyclic Behaviour of Expanded Polystyrene (EPS) Sandwich Reinforced Concrete Walls

Ari Wibowo, Indradi Wijatmiko, and Christin R. Nainggolan

Department of Civil Engineering, Faculty of Engineering, Brawijaya University, Malang 65149, Indonesia

Correspondence should be addressed to Ari Wibowo; ariwibowo@ub.ac.id

Received 31 May 2018; Revised 12 October 2018; Accepted 8 November 2018; Published 26 December 2018

Academic Editor: Pietro Russo

Precast concrete walls become increasingly utilized due to the rapid needs of inexpensive fabricated house especially as traditional construction cost continues to climb, and also, particularly at damaged area due to natural disasters when the requirement of a lot of fast-constructed and cost-efficient houses are paramount. However, the performance of precast walls under lateral load such as earthquake or strong wind is still not comprehensively understood due to various types of reinforcements and connections. Additionally, the massive and solid wall elements also enlarge the building total weight and hence increase the impact of earthquake significantly. Therefore, the precast polystyrene-reinforced concrete walls which offer light weight and easy installment became the focus of this investigation. The laboratory test on two reinforced concrete wall specimens using EPS (expanded polystyrene) panel and wire mesh reinforcement has been conducted. Quasi-static load in the form of displacement controlled cyclic tests were undertaken until reaching peak load. At each discrete loading step, lateral load-deflection behaviour, crack propagation, and collapse mechanism were measured which then were compared with theoretical analysis. The findings showed that precast polystyrene-reinforced concrete walls gave considerable seismic performance for the low-to-moderate seismic region reaching up to 1% drift at 20% drop of peak load. However, it might not be sufficient for high seismic regions, at which double-panel wall type can be more suitable.

1. Introduction

Tall buildings particularly with irregularities are prone to behave poorly and collapse when subjected to lateral loads such as earthquake excitation or strong wind. To overcome this problem, shear walls are commonly preferable to increase the lateral strength of structures significantly. However, the added massive and solid shear walls result in increasing the building weight and consequently the base shear due to earthquake excitation which might reduce the effectiveness of the shear wall use in the structures. The effort to reduce the weight of shear walls without losing lateral strength capacity is necessary.

There were many studies investigating lightweight concrete shear walls with various techniques to reduce the element weight such as using lightweight aggregates, applying porous concrete system, or inserting lightweight panel into the wall. Mousavi et al. [1] studied the effectiveness of the JK system wall, composed of EPS concrete (mortar with EPS beads as fine aggregates) and galvanized steel reinforcement, in sustaining lateral load. It was observed that JK walls had high ductility capacity, but still need further observation for the application in tall and medium buildings. Yizhou [2] investigated that the use of gangue as an aggregate in concrete shear wall provided larger energy dissipation compared with normal concrete shear wall. Furthermore, Hejin et.al. [3] focused on ash ceramsite as alternative for lightweight aggregate concrete shear wall which gave similar load-deflection behaviour and collapse mechanism to those on normal concrete ones, whereas Chai and Anderson [4] found that the performance of concrete wall panels using perforated lightweight aggregate in low-rise buildings subjected to lateral forces was generally satisfactory. Cavaleri et al. [5] investigated pumice stone in comparison with expanded clay and normal stone as aggregates in concrete shear wall which showed the benefit of the use pumice stones.

On the other side, reducing the weight of structural elements can be achieved using the sandwich system by

inserting a lightweight panel inside the concrete element. This panel system is usually applied for insulation purpose as well. The lightweight wall system investigated in this paper focused on the use of the EPS panel as a filler and galvanized wire mesh for reinforcing bar as shown in Figure 1.

2. Research Methodology

The specimens were designed as structural walls composing low-rise building which were commonly found in house or school precast buildings. The squat walls are generally dominated with shear behaviour which comparably differs to tall walls commonly found in high-rise building. Concrete tall walls have been considerably well-researched and well-understood [7–10], whereas concrete squat walls have been increasingly investigated [11–14]. However, innovation studies on sandwich squat walls with the EPS panel were just initially begun. Previous experimental studies by Trombetti et al. [15] and Ricci et al. [16] showed that sandwich squat concrete walls were comparable to those of regular RC walls and able to sustain lateral load up to drift higher than 1.3%, whereas Palermo and Trombetti [17] comprehensively investigated sandwich walls experimentally and analytically with the outcomes showed that properly designed walls can accomplish high seismic performance requirement suggested by the code. However, the overall performance of sandwich RC walls with lower steel reinforcement ratios (less than minimum requirements) still needs further investigation and hence became the main focus of this study.

The laboratory tests on two specimens of sandwich reinforced concrete wall RCW4 and RCW8 have been undertaken. Figure 2 shows the typical property of the walls. All specimens had a height and width of 90 cm and 60 cm, respectively (equivalent to aspect ratio of 1.5). The RCW4 wall used a 4 cm thick EPS panel compared to the 8 cm EPS panel installed in the RCW8 wall. The specimens were reinforced with ϕ2.5–75 mm wire mesh on each wall side and ϕ3.0 mm steel wires for connecting both mesh layers. The yield and ultimate steel tensile strengths of the wire mesh were 600 MPa and 680 MPa, respectively, as shown in Figure 3. A 35 mm thick shotcrete was applied on each outer side of walls with the concrete strength of 15 MPa. The walls and the foundations were connected using ϕ10 mm anchor bars spaced at 75 mm.

Quasi-static cyclic load procedure was applied at the tip of the wall specimens to obtain representative hysteretic curves of lateral load versus displacement (refer Figures 4 and 5) as per ASTM E2126 code [18]. The drift-controlled order was used for the loading test comprised drift increments of 0.042% until attaining 0.167% (representing cracking point), then drift increments of 0.16% until reaching drift of 0.66% (representing yield point), and followed by inelastic stage at 0.66% drift increments. The hysteretic behaviours of walls were maintained using three loading cycles at each drift ratio.

During the testing process, at each defined discrete displacement stages, the measurement of LVDTs, dial gauges, and crack propagation were recorded. The test stopped when the peak lateral strength of the specimen reduced by 20% (lateral load failure).

3. Experimental Test Results

Hysteretic curves of lateral load-drift relationship and the crack pattern of all wall specimens are presented in Figure 6. Both specimens RCW4 and RCW8 had similar peak lateral load of about 25 kN with different behaviour characteristics. RCW4 (EPS panel thickness of 40 mm) developed more classical flexural mechanism, whilst RCW8 (EPS panel thickness of 80 mm) was more dominated with yield penetration behaviour due to the thinner concrete cover of wall foundation. As shown, the specimen RCW4 managed to complete all three cycles of quasi-static cyclic load at 1.0% drift, and then failed at the first cycle of load at drift of 1.33%, whereas specimen RCW8 produced shorter maximum drift capacity with failure at the first cycle of lateral load at 1.0% drift. A comparison of lateral strengths and drifts between the experimental results and the theoretical predictions is presented in Table 1.

The total lateral deformation consists of flexural, shear, and yield penetration components that were determined using dial gauge and LVDT and dial gauge measurements as shown in Figure 7.

The flexural displacement at the wall top at each i-segment of LVDT was determined via the following equation (refer Figure 7(a)):

$$\Delta_{\mathrm{fl}.i} = \int_0^L \varphi(x)x\,dx = \frac{L - L_{\mathrm{vi}}}{L_{\mathrm{h}}}\left(\delta_{\mathrm{f2}} - \delta_{\mathrm{f1}}\right), \tag{1}$$

whereas the displacement of the elastic region at upper segment was estimated analytically assuming uncracked section properties as follows:

$$\Delta_{\mathrm{fl}.3} = \frac{\varphi L_i^2}{3} = \frac{FL_i^3}{3E_{\mathrm{c}}I}, \tag{2}$$

where F = lateral load; L_i = segment length; E_{c} = concrete elastic modulus; and I = uncracked moment of inertia.

The shear deformation Δ_{sh} was predicted using diagonal LVDTs data (refer Figure 7(b)) as follows:

$$\Delta_{\mathrm{sh}} = \frac{\left(\delta_{\mathrm{s1}} - \delta_{\mathrm{s2}}\right)}{2}\sec\xi = \frac{\left(\delta_{\mathrm{s1}} - \delta_{\mathrm{s2}}\right)}{2}\,\frac{\sqrt{L_{\mathrm{v}}^2 + D^2}}{L_{\mathrm{v}}}, \tag{3}$$

where D = wall depth and $\delta_{\mathrm{s}i}$ = diagonal LVDT measurement.

The yield penetration component was measured using the vertical LVDT at the first level (refer Figure 7(c)) by assuming a rocking mechanism within the first section of wall. An upper bound of the top displacement of the column can be calculated from the product of the slip rotation θ_{slip} and the column height assuming rigid body rotation as follows:

$$\Delta_{\mathrm{yp}} = \theta_{\mathrm{slip}} L_{\mathrm{column}}, \tag{4}$$

where θ_{slip} = the slip rotation of tensile steel = $(\delta_{\mathrm{slip}}/(d-c)) \approx \beta$; $\beta = ((\delta_{\mathrm{f2}} - \delta_{\mathrm{f1}})/L_{\mathrm{h}})$ and c = the neutral axis depth at the column base interface = $(\delta_{\mathrm{f2}}/(\delta_{\mathrm{f1}} + \delta_{\mathrm{f2}}))L_{\mathrm{h}} - d_2$.

The deformation of walls comprising flexural, shear, and yield penetration components for RCW4 and RCW8 specimens is shown in Figure 8. The flexural deformation was the most dominant component of about 75% and 55%

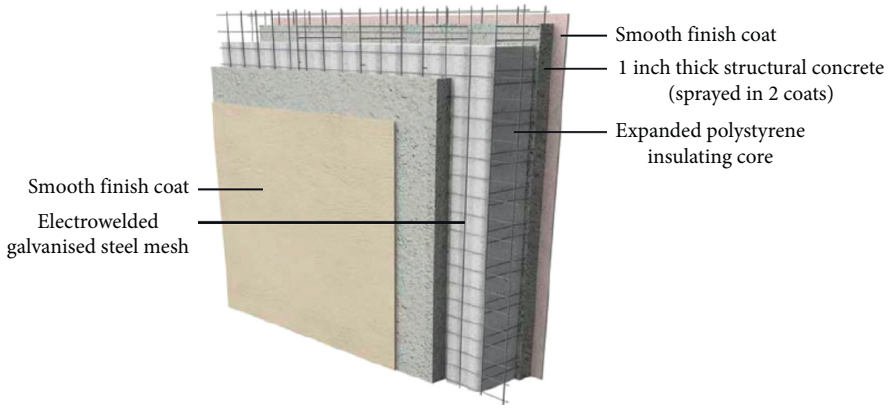

Figure 1: Typical EPS sandwich concrete wall panel (refer [6]).

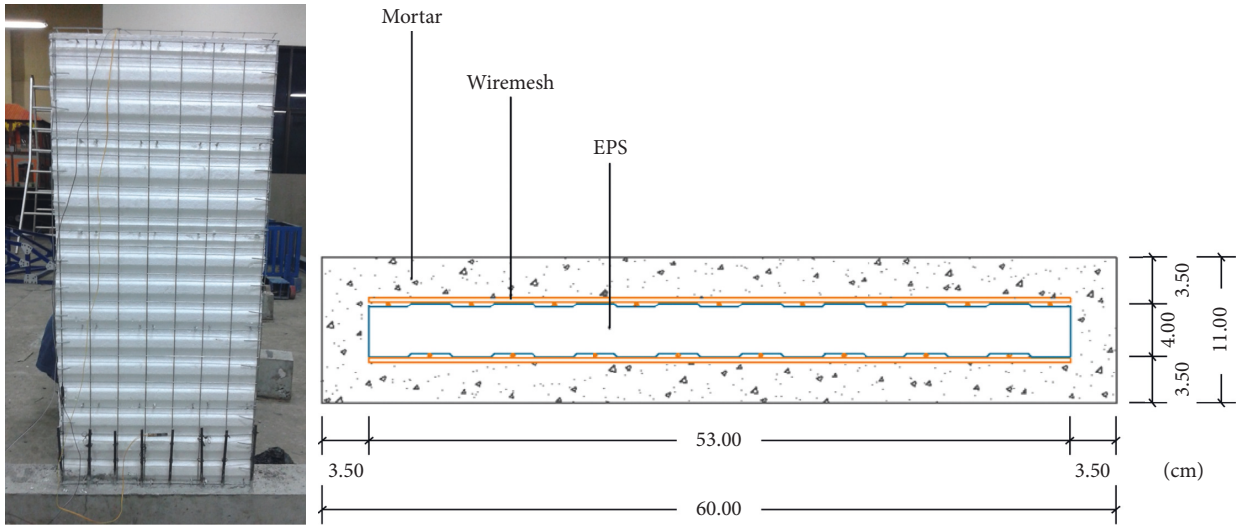

Figure 2: Basic properties of wall specimens.

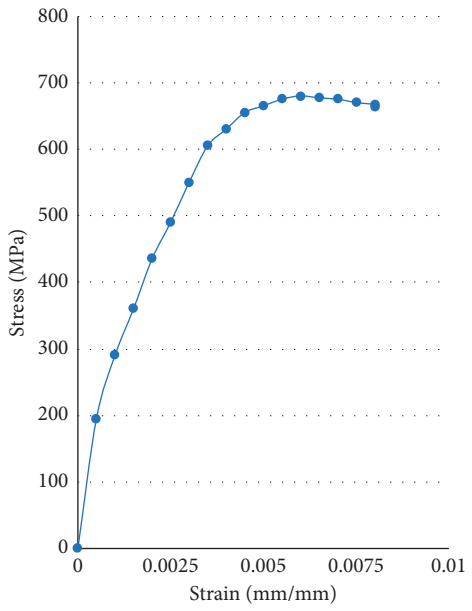

Figure 3: Stress-strain relationship of steel wire.

for RCW4 and RCW8 specimens, respectively, whilst, the shear deformation was the least dominant deformation component of below 5% for both specimens RCW4 and RCW8. Interestingly, the yield penetration deformation of RCW8 was about 27% compared to 21% of that of RCW4 specimen, which can be attributed to the smaller concrete cover of sloof foundation on RCW8 and hence smaller bond slip strength between steel bar and concrete at foundation.

4. Backbone Curve Models

Two simple models (backbone and simplified) were developed for design purposes or basic assessment of lateral load-displacement capacity of such walls. Both models for sandwich concrete walls are developed based on the model previously developed by authors for lightly reinforced concrete walls [19].

4.1. Model 1: Detailed. A detailed curve model is developed based on displacement-based design methodology for predicting the lateral load-drift behaviour (comprising four stages: cracking, yield, peak, and lateral load failure) as shown conceptually in Figure 9.

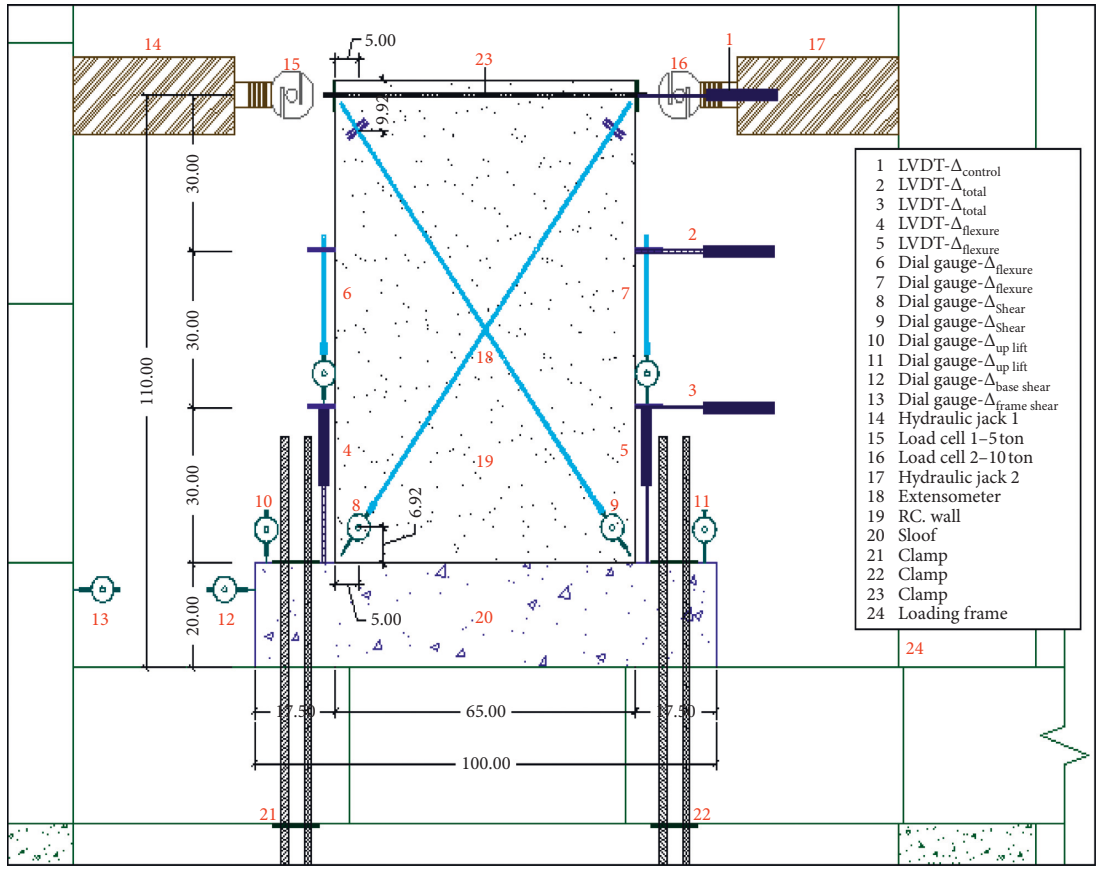

Figure 4: Schematic of wall loading test setup.

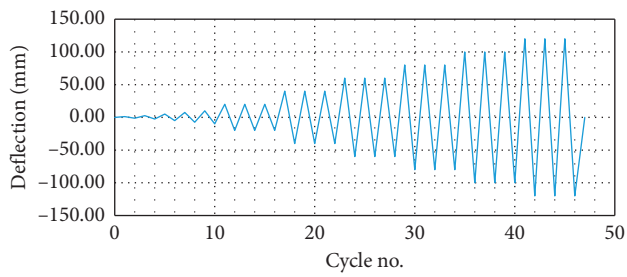

Figure 5: Quasi-static lateral loading history.

(a) Point A (cracking): the cracked lateral strength and drift are calculated as follows:

$$F_{cr} = \frac{M_{cr}}{L},$$
$$\gamma_{cr} = \frac{M_{cr}L}{3E_cI_g}, \tag{5}$$

where the flexural tensile strength f_t is taken as $0.6\sqrt{f'_c}$.

(b) Point B (yield): the yield drift is calculated using the effective second moment of area as follows:

$$F_y = \frac{M_y}{L},$$
$$\gamma_y = \frac{M_yL}{3E_cI_e}. \tag{6}$$

The Paulay and Priestley [8] model for effective moment of inertia is used as follows.

(i) Flexure-dominated walls:

$$I_e = \left(\frac{100}{f_y} + \frac{P_u}{f'_cA_g}\right)I_g. \tag{7}$$

(ii) Shear-dominated walls:

$$I_w = \frac{I_g}{1.2 + C},$$
$$C = \frac{30I_e}{L^2tD}, \tag{8}$$

where P_u = nominal axial load, A_g = gross cross section area of walls, and t = wall thickness.

(c) Point C (peak strength): the model was developed by investigating the curvature within the plastic hinge region using the force equilibrium equation ($N = C_c + C_s - T$) with the spalling strain ($\varepsilon_{cu} = 0.003$) used as a limit state for concrete strain. For low-rise buildings, the presence of gravity axial load is reasonably small, and hence for simplicity, the compression steel area is eliminated from the equilibrium equation. The peak flexural lateral load F_u and the drift at concrete fracture γ_u can then be obtained as follows:

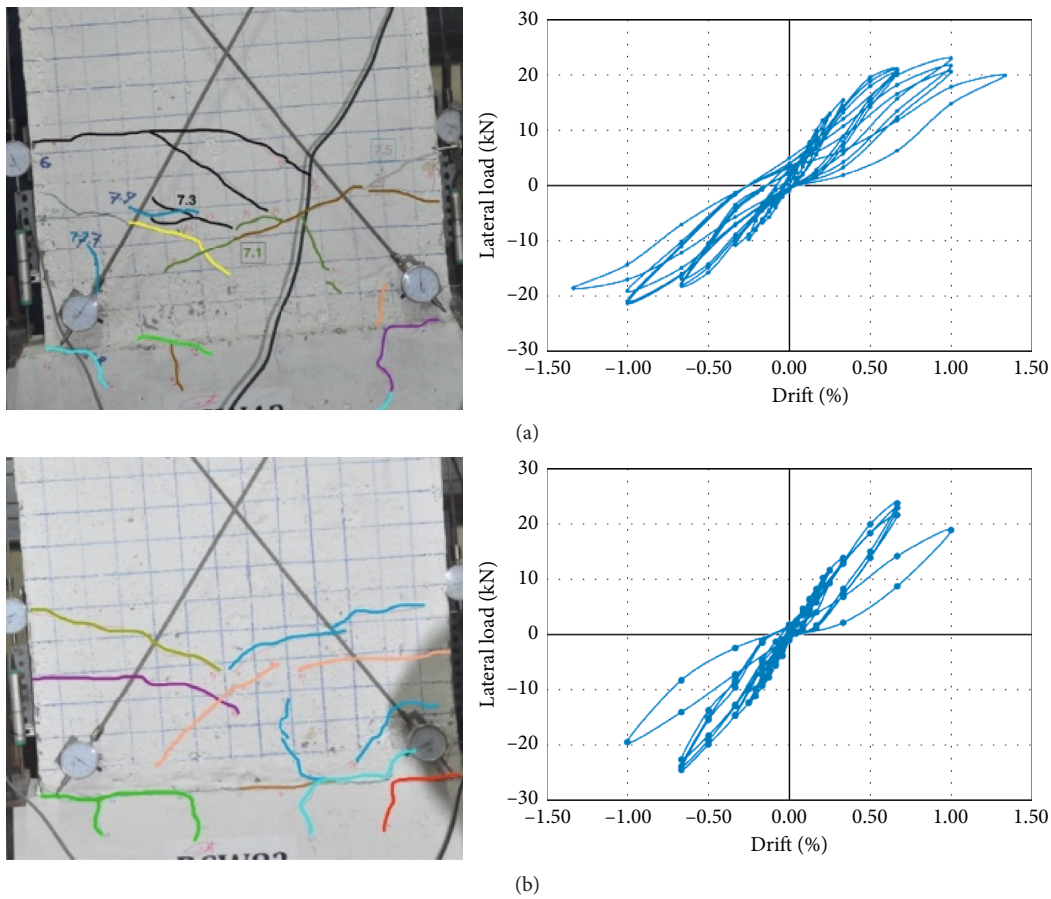

Figure 6: Crack patterns at 1% drift and hysteretic curves of all specimens: (a) RCW4; (b) RCW8.

Table 1: Strength and deformation properties of specimens RCW4 and RCW8.

		Strength (kN)			Drift (%)			
		F_{cr}	F_y	F_u	δ_{cr}	δ_y	δ_u	δ_{lf}
RCW4	Exp.	2.8	18	23.5	0.17	0.47	1.00	1.33
	Theo.	4.0	16	23	0.1	0.42	0.75	n.a
RCW8	Exp.	2.3	20	24.5	0.17	0.55	0.67	1.00
	Theo.	4.3	18	23.5	0.1	0.43	0.8	n.a

Note. The theoretical values were taken from moment-curvature analysis (flexural component only).

$$F_u = \frac{M_u}{L},$$
$$\gamma_{peak} = \gamma_y + \gamma_{pl\cdot p}, \tag{9}$$

where $\gamma_{pl\cdot p} = (\phi_{peak} - \phi_y)L_p$ in which $\phi_{peak}(\varepsilon_{cu}/k_u d) = (0.003/k_u d)$ and $\phi_y = (3\gamma_y/L)$, $k_u = ((N + A_{st}f_y)/0.85 f'_c \gamma d b)$, $\gamma = 0.85 - 0.007(f'_c - 28)$, A_{st} = tensile steel area, and ε_{sm} = steel strain-hardening strain.

The plastic hinge length L_p can be estimated using the Paulay and Priestley model [8] as follows:

$$L_p = 0.054L + 0.022\, d_b f_y. \tag{10}$$

(d) Point D (ultimate displacement): lateral load-displacement relationship of squat walls is dominated by shear behaviour; however, for lightly reinforced squat walls, the flexure behaviour still provides large influence on lateral load-drift behaviour. The failure mechanism which is influenced by shear strength degradation is needed; hence, the lateral load failure models developed for lightly reinforced concrete columns and walls [20, 21] are modified for this model due to the similarity of lateral load-displacement behaviour between lightly reinforced concrete walls and columns.

Shear strength (V_u) of RC walls consists of concrete strength (V_c) and steel strength (V_s) components as follows:

$$V_u = V_c + V_s. \tag{11}$$

In this model, the concrete shear strength uses the formula developed based on principal tensile strength by authors [22], whilst the steel strength proposed by Wesley and Hashimoto [23] is used as follows:

$$V_c = \frac{2}{3}A_{cr}\sqrt{(f_t)^2 + \frac{f_t P}{A_{cr}}}, \tag{12}$$

$$V_s = (c_h\rho_h + c_v\rho_v) f_y dt, \tag{13}$$

where

$$A_{cr} = 0.85(n_c\rho_{st})^{0.36} dt, \tag{14}$$

where d is the effective depth of RC walls, which can be assumed as $0.8D$, and $C_h = 1 - c_v$, in which

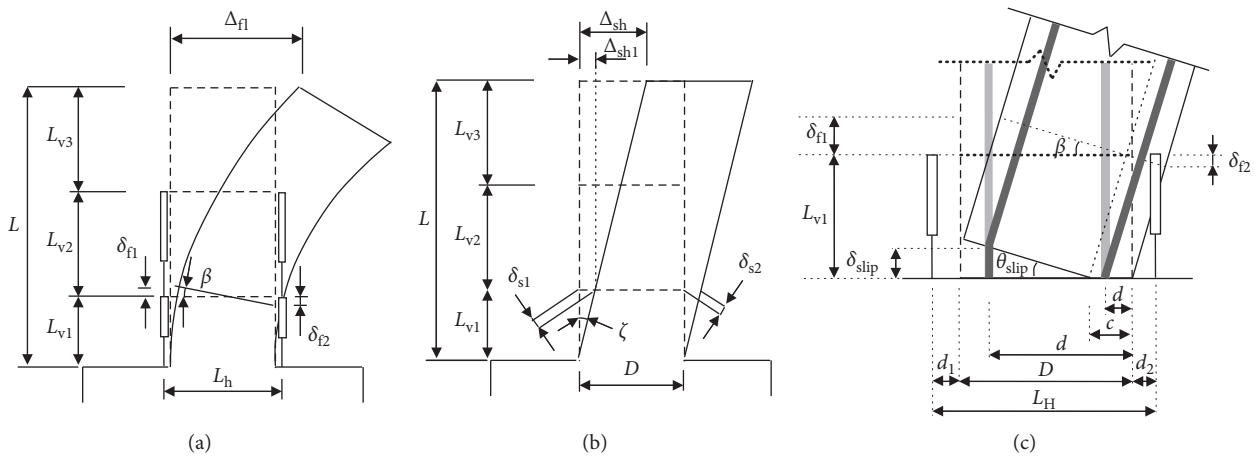

Figure 7: LVDT measurements for (a) flexure deformation, (b) shear deformation, and (c) yield penetration deformation.

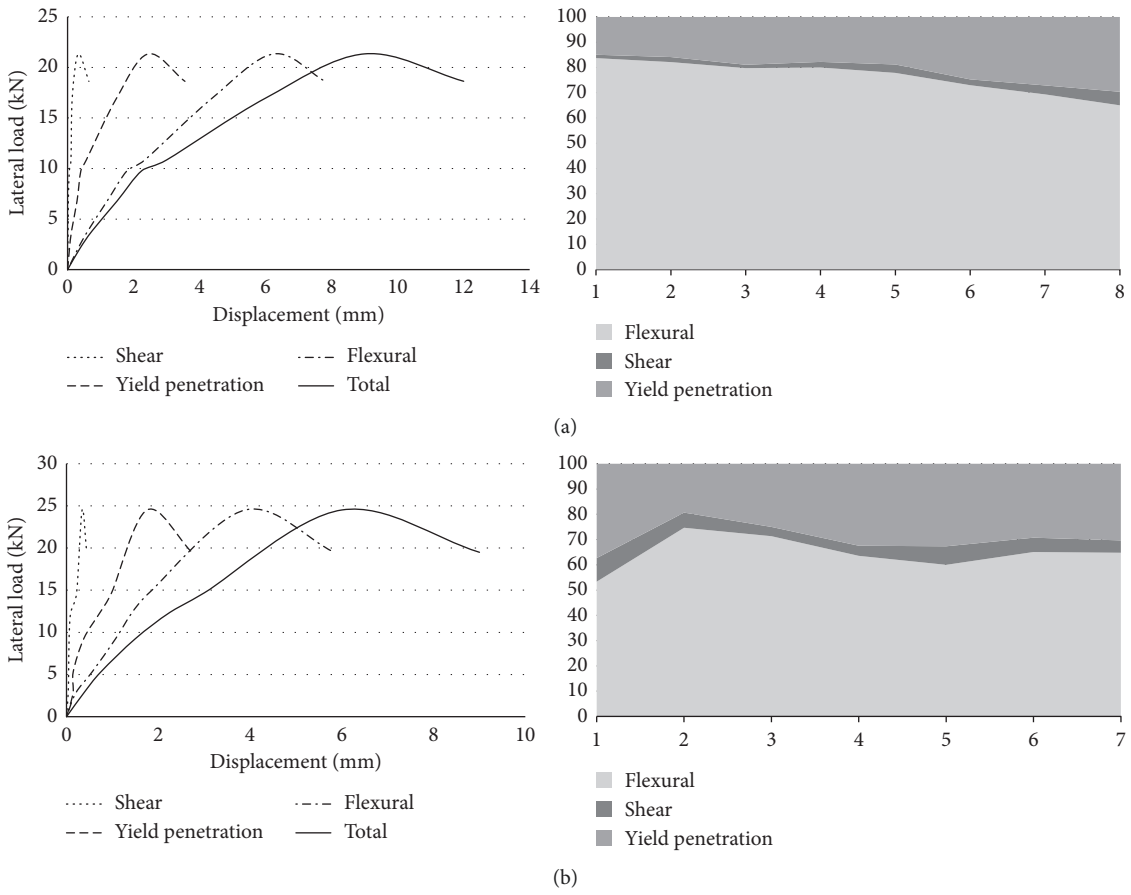

Figure 8: Variation of displacements due to flexure, shear, and yield penetration: axial load-deformation relationship (left) and ratio of each displacement to total displacement at each loading step (right). (a) RCW4 specimen. (b) RCW8 specimen.

$$c_v = 1, \quad \text{for } a < 0.5$$
$$= 2(1-a), \quad \text{for } 0.5 < a < 1 \qquad (15)$$
$$= 0, \quad \text{for } a > 1,$$

with $n_c = E_s/E_c$, ρ_h = the transverse reinforcement ratio, ρ_v = the total longitudinal reinforcement ratio, and ρ_{st} = the tension reinforcement ratio.

As a note, for moderate and slender walls ($a > 1$, and hence $c_v = 0$), the steel strength component (equation (13)) can be rewritten as a common shear strength formula:

$$V_s = \rho_h f_y dt = \frac{A_v f_y d}{s}. \qquad (16)$$

The ultimate drift can be obtained as follows:

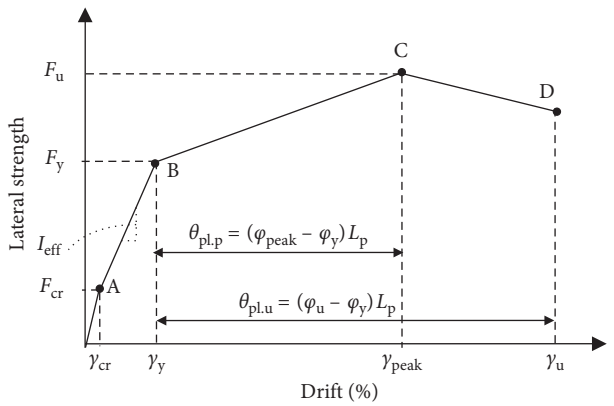

Figure 9: The backbone curve model of lateral load-drift capacity [20].

$$\gamma_u = \frac{\gamma_y}{k}\left[(1 - k\alpha) - 0.8\frac{F_u}{V_u}\right], \tag{17}$$

where

$$k = \frac{0.3e^{5.7n}}{9 - a}, \tag{18}$$

where α = the drift ductility at the start of shear strength decrease.

4.2. Model 2: Simplified. The simplified model is a simple procedure for estimating lateral load-drift behaviour of lightly reinforced concrete walls. This model consists of trilinear stages with each state: cracking, yield, and ultimate as shown in Figure 10.

(a) Point A (cracking): the lateral strength at cracking point can be predicted by assuming cracking drift γ_{cr} = 0.05%.

(b) Point B (yield): the ultimate yield strength is calculated using factored ultimate strength:

$$F_y = \phi F_u, \tag{19}$$

whereas the corresponding yield drift (γ_y) is determined using the smallest values of the following alternatives:

(i) Approximate value of γ_y = 0.2%–0.3%

(ii) Apply $I_{eff} = 0.5I_g$ (refer [24])

(c) Point C (ultimate): the ultimate drift (γ_m) can be calculated as a sum of the yield drift (γ_y) and the plastic drift (γ_{pl}) as follows (refer Figure 11):

$$\gamma_m = \gamma_y + \gamma_{pl}. \tag{20}$$

The plastic drift can be estimated by assuming a maximum acceptable strain in the steel bar at single crack at the wall base in the order of ε_s = 5.0% and taking a more conservative approach to Priestley and Paulay [8] strain penetration length of $l_{yp} = 4400\ \varepsilon_y\ d_b \approx 15d_b$. Hence, the following models can be obtained (refer Figure 12).

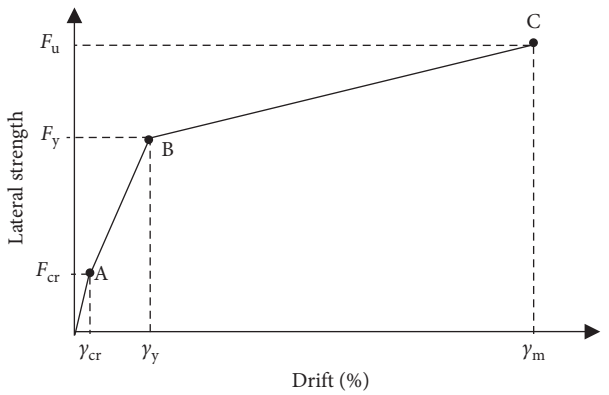

Figure 10: The simplified model of lateral load-drift capacity.

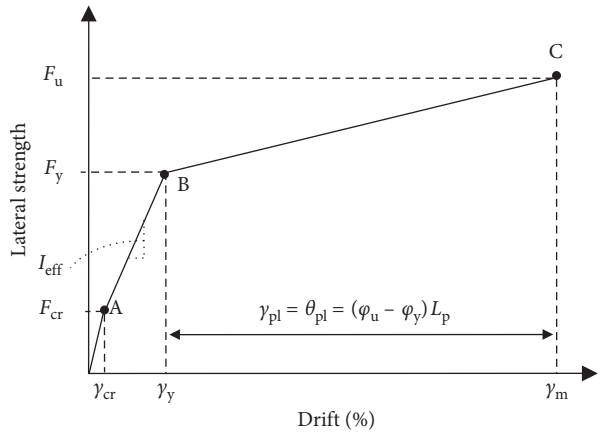

Figure 11: Plastic drift of simplified model.

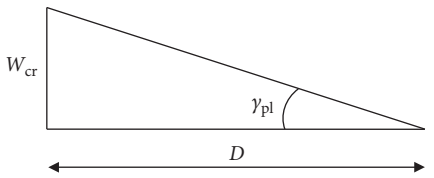

Figure 12: Plastic rotation at wall base.

Crack width:

$$W_{cr} = \varepsilon_s \cdot l_{yp} = 0.05 \times 15d_b = 0.75d_b, \tag{21}$$

Plastic drift:

$$\gamma_{pl} = \theta_{pl} = \frac{w_{cr}}{D} = 0.75\left(\frac{d_b}{D}\right). \tag{22}$$

The lateral load-drift relationship between experimental data and proposed models are considerably in good agreement as shown in Figures 13 and 14. More data are certainly required to refine the models particularly for the detailed model since it was developed using a semiempirical approach. However, interestingly, the simplified model with the pure analytical approach showed better prediction due to the dominant combinations of flexural and yield penetration behaviour.

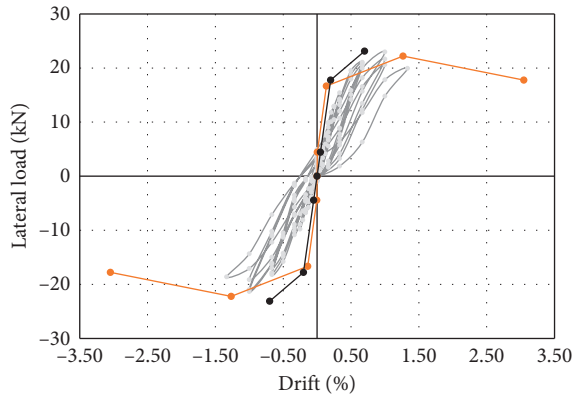

Figure 13: Comparison between experimental data and theoretical models for specimen RCW4.

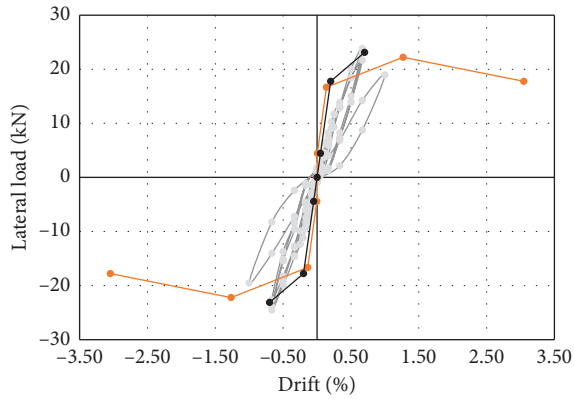

Figure 14: Comparison between experimental data and theoretical models for specimen RCW8.

5. Conclusion

Two specimens of light-weight sandwich concrete walls have been tested in order to investigate the lateral load-drift behaviour and collapse mechanism. Specimen RCW4 with a thinner EPS panel developed more classic flexural behaviour with drift capacity maxed at about 1.3%, whilst specimen RCW8 only managed to reached 1.0% with dominant yield penetration behaviour due to thinner concrete cover of sloof foundation. However, the tests were stopped at 20% drop of peak load instead of further failure at axial load collapse. And, hence the results can still be considered satisfactory for low-to-moderate seismic regions but might not be sufficient for high seismic regions.

Two models comprising detailed and simplified approach for predicting the load-displacement behaviour of sandwich concrete wall subjected to lateral load have been developed. The experimental data and the proposed models are in good agreement, particularly the simplified model due to the dominant behaviour of flexural and yield penetration.

Data Availability

The data that support the findings of this study are available from the corresponding author upon reasonable request.

Conflicts of Interest

The authors declare that they have no conflicts of interest.

References

[1] S. A. Mousavi, S. M. Zahrai, and A. Bahrami-Rad, "Quasi-static cyclic tests on super-lightweight EPS concrete shear walls," *Engineering Structures*, vol. 65, pp. 62–75, 2014.

[2] Z. Yizhou, "Mechanical properties of self-combusted gangue reinforced concrete shear walls under low-cyclic load," *Journal of Zhejiang University, Engineering Science*, vol. 34, no. 3, pp. 325–330, 2000.

[3] T. Hejin, Y. Qingrong, and S. Xinya, "Experimental study on bBehaviours of reinforced ash ceramsite concrete shear walls," *Journal of Building Structure*, vol. 15, no. 4, pp. 20–30, 1994.

[4] Y. H. Chai and J. D. Anderson, "Seismic response of perforated lightweight Aggregate concrete wall panels for low-rise modular classrooms," *Engineering Structures*, vol. 27, no. 4, pp. 593–604, 2005.

[5] L. Cavaleri, N. Miraglia, and M. Papia, "Pumice concrete for structural wall panels," *Engineering Structures*, vol. 25, no. 1, pp. 115–125, 2003.

[6] http://mpanelindonesia.com/product/wall-panel/.

[7] T. Paulay, "Earthquake-resisting shear walls-New Zealand design trends," *ACI Journal*, vol. 77, no. 18, pp. 144–152, 1980.

[8] T. Paulay and M. J. N. Priestley, *Seismic Design of Reinforced Concrete and Masonry Buildings*, Wiley Interscience Press publication, John Wiley & Sons inc., New York City, NY, USA, 1992.

[9] O. Esmaili, S. Epackachi, M. Samadzad et al., "Study of structural RC shear wall system in a 56-story RC tall building," in *Proceedings the 14th World Conference on Earthquake Engineering*, Beijing, China, October 2008.

[10] A. Carpinteri, M. Corrado, G. Lacidogna et al., "Lateral load effects on tall shear wall structures of different height," *Structural Engineering and Mechanics*, vol. 41, no. 3, pp. 313–337, 2012.

[11] P. A. Hidalgo, C. A. Ledezma, and R. M. Jordan, "Seismic bBehaviour of squat reinforced concrete shear walls," *Earthquake Spectra*, vol. 18, no. 2, pp. 287–308, 2002.

[12] T. N. Salonikios, "Shear strength and deformation patterns of R/C walls with aspect ratio 1.0 and 1.5 designed to Eurocode 8," *Engineering Structures*, vol. 24, no. 1, pp. 39–49, 2002.

[13] T. N. Salonikios, "Analytical prediction of the inelastic response of RC walls with low aspect ratio," *ASCE Journal of Structural Engineering*, vol. 133, no. 6, pp. 844–854, 2007.

[14] J. Carrillo and S. M. Alcocer, "Shear strength of reinforced concrete walls for seismic design of low-rise housing"," *ACI Structural Journal*, vol. 110, no. 3, 2013.

[15] T. Trombetti, G. Gasparini, S. Silvestri et al., "Results of pseudo-static tests with cyclic horizontal load on cast in situ sandwich squat concrete walls," in *Proceedings of Ninth Pacific Conference on Earthquake Engineering Building an Earthquake-Resilient Society*, Auckland, New Zealand, April 2011.

[16] I. Ricci, M. Palermo, G. Gasparini, S. Silvestri, and T. Trombetti, "Results of pseudo-static tests with cyclic horizontal load on cast in situ sandwich squat concrete walls," *Engineering Structures*, vol. 54, pp. 131–149, 2013.

[17] M. Palermo and T. Trombetti, "Experimentally-validated modelling of thin RC sandwich walls subjected to seismic loads," *Engineering Structures*, vol. 119, pp. 95–109, 2016.

[18] ASTM E2126, *Standard Test Methods for Cyclic (Reversed) Load Test for Shear Resistance of Walls for buildings*, ASTM International, West Conshohocken, PA, USA, 2005.

[19] A. Wibowo, J. L. Wilson, N. T. K. Lam et al., "Seismic performance of lightly reinforced structural walls for design purposes," *Magazine of Concrete Research*, vol. 65, no. 13, pp. 809–828, 2013.

[20] J. L. Wilson, A. Wibowo, N. T. K. Lam et al., "Drift behaviour of lightly reinforced concrete columns and structural walls for seismic design applications," *Australian Journal of Structural Engineering*, vol. 16, no. 1, pp. 62–74, 2015.

[21] A. Wibowo, J. L. Wilson, N. T. K. Lam et al., "Drift performance of lightly reinforced concrete columns," *Engineering Structures*, vol. 59, pp. 522–535, 2014.

[22] A. Wibowo, J. L. Wilson, N. T. K. Lam et al., "Drift capacity of lightly reinforced concrete columns," *Australian Journal of Structural Engineering*, vol. 15, no. 2, pp. 131–150, 2014.

[23] D. A. Wesley and P. S. Hashimoto, "Seismic structural fragility investigation for the zion nuclear power plant," Report NUREG/CR-2320, US Nuclear Regulatory Commission, Bethesda, MD, USA, 1981.

[24] J. W. Wallace, "Modelling issues for tall reinforced concrete core wall buildings," *The Structural Design of Tall and Special Buildings*, vol. 16, no. 5, pp. 615–632, 2007.